Medicine®

OPEN

Thoracic [18F]fluorodeoxyglucose uptake measured by positron emission tomography/computed tomography in pulmonary hypertension

Armin Frille (MD)[a],[*], Karen Geva Steinhoff (MD)[b], Swen Hesse (MD)[b],[c], Sabine Grachtrup (MD)[a], Alexandra Wald (MD)[a], Hubert Wirtz (MD)[a], Osama Sabri (MD)[b], Hans-Juergen Seyfarth (MD)[a]

Abstract

Positron emission tomography (PET) visualizes increased cellular [18F]fluorodeoxyglucose ([18F]FDG) uptake. Pulmonary hypertension (PH) is conceived of a proliferative disease of the lung vessels. Increased glucose uptake can be quantified as pulmonary [18F]FDG uptake via PET imaging. Because the angioproliferative mechanisms in PH are still in need of further description, the aim of the present study was to investigate whether [18F]FDG PET/CT imaging can elucidate these pathophysiologic mechanisms in different etiologies of PH.

Patients (n = 109) with end-stage pulmonary disease being evaluated for lung transplant were included in this observational study. Mean standardized uptake value (SUV_{mean}) of predefined regions of interest in lung parenchyma (LP), left (LV), and right ventricle (RV) of the heart, and SUV_{max} in pulmonary artery (PA) were determined and normalized to liver uptake. These SUV ratios (SUVRs) were compared with results from right heart catheterization (mean pulmonary artery pressure [mPAP], pulmonary vascular resistance [PVR]), and serum N-terminal pro-brain natriuretic peptide. Group comparisons were performed and Pearson correlation coefficients (r) were calculated.

The [18F]FDG uptake ratios in LP, RV, RV/LV, and PA, but not in LV, were found to be significantly higher in both patients with mPAP ≥25 mm Hg ($P = 0.013$, $P = 0.006$, $P = 0.049$, $P = 0.002$, $P = 0.68$, respectively) and with PVR ≥480 dyn·s/cm^5 ($P < 0.001$, $P = 0.045$, $P < 0.001$, $P < 0.001$, $P = 0.26$, respectively). The [18F]FDG uptake in these regions positively correlated also with mPAP, PVR, and N-terminal pro-brain natriuretic peptide. The SUVR of PA positively correlated with the SUVR of LP and RV ($r = 0.55$, $r = 0.42$, respectively).

Pulmonary and cardiac [18F]FDG uptake in PET imaging positively correlated with the presence and severity of PH in patients with end-stage pulmonary disease. Increased glucose metabolism in the central PAs seems to play a certain role in terms of severity of PH. These results suggest that [18F]FDG-PET imaging can help understand the pathophysiology of PH as a proliferative pulmonary disease.

Abbreviations: [18F]FDG PET = [18F]fluorodeoxyglucose positron emission tomography, 6MWD = 6-minute walking distance, CI = confidence interval, CO = cardiac output, COPD = chronic obstructive lung disease, CRP = C-reactive protein, CT = computed tomography, CTEPH = chronic thromboembolic pulmonary hypertension, i.v. = intravenous, ILD = interstitial lung disease, IPAH = idiopathic pulmonary arterial hypertension, ln = natural logarithm to the base e, LP = lung parenchyma, LV = left ventricle, mPAP = mean pulmonary artery pressure, n = number of patients, NT-proBNP = N-terminal pro-brain natriuretic peptide, PA = pulmonary artery, PAH = pulmonary arterial hypertension, PCWP = pulmonary capillary wedge pressure, PH = pulmonary hypertension, PVR = pulmonary vascular resistance, RHC = right heart catheterization, ROI = region of interest, RV = right ventricle, SD = standard deviation, SUV = standardized uptake value, SUVR = standardized uptake value ratio, VOI = volume of interest, WBC = white blood cell.

Keywords: positron emission tomography, pulmonary end-stage disease, pulmonary glucose uptake, pulmonary hypertension

1. Introduction

Pulmonary hypertension (PH) is a disease characterized by a progressive vascular remodeling leading to chronically elevated pulmonary vascular resistance (PVR) and pulmonary arterial pressure. By definition, the mean pulmonary artery pressure (mPAP) at rest is invasively measured $\geq$25 mm Hg.[1] According to the updated clinical classification of PH established at the fifth World Symposium on PH in 2013, PH is classified into 5 functional groups depending on the etiology of PH.[1] Briefly, PH may be due to (1) a pulmonary arterial hypertension (PAH) including idiopathic, familial, drug, and toxin-induced and associated forms; (2) due to left heart diseases; (3) due to lung diseases and/or hypoxia, for example, chronic obstructive lung diseases (COPDs) and interstitial lung diseases (ILDs); (4) due to chronic thromboembolic PH (CTEPH); and (5) due to unclear multifactorial mechanisms (hematologic, systemic, or metabolic disorders). Since clinical presentation remains rather unspecific, PH is unfortunately diagnosed at an advanced stage. Until now, the gold standard has been the right heart catheterization (RHC) to establish diagnosis and to assess severity of PH.

Current perceptions of cellular and molecular mechanisms leading to PH comprise of angioproliferative events in the lung parenchyma.[2] Loss of growth control and a glycolytic shift towards aerobic cytoplasmic glycolysis similar as in cancer cells have been observed in animal and human model studies investigating the pathophysiology of PH.[3–6] The fact that under normal oxygen supply predominantly glycolysis rather than mitochondrial oxidation for adenosine triphosphate generation is performed leads to an increased glucose uptake, also known as Warburg effect.[7]

Positron emission tomography (PET) using ^{18}F-labeled tracer fluorodeoxyglucose (FDG) represents an established tool in oncology for diagnosing, staging disease, prognostic stratification, and monitoring therapy.[8] But also nonmalignant proliferative cells like pulmonary endothelial and smooth muscle cells, and also fibroblasts in experimental PH models, are believed to utilize aerobic glycolysis.[3,5,9]

Increased [^{18}F]FDG uptake in lung parenchyma of patients with idiopathic PAH compared with a healthy control group was found by using PET imaging.[5,10]

By now, only 4 clinical PET studies are known to us having investigated the influence of [^{18}F]FDG uptake in the lungs of altogether 54 patients with PH.[5,9–11] Those patients under investigation suffered primarily from severe PAH (48/54, 88.9%) and from CTEPH (6/54, 11.1%). The role of pulmonary and cardiac [^{18}F]FDG uptake in patients with PH due to pulmonary disease (World Health Organization group 3) has not yet been investigated.

Therefore, the aim of this study was to assess pulmonary and cardiac [^{18}F]FDG uptake measured with PET/CT in patients referred for lung transplant evaluation due to end-stage pulmonary disease. We hypothesize that pulmonary and cardiac [^{18}F]FDG uptake may help understand the pathophysiology of PH as a proliferative pulmonary disease.

2. Material and methods

2.1. Patient characteristics

In this observational (cross-sectional) study, 109 patients were included (66 men, 43 women; mean age $\pm$ standard deviation (SD) 54.4 $\pm$ 7.5 years). Patients were referred for lung transplant evaluation due to end-stage pulmonary disease, from September 2007 to January 2015. This retrospective study received approval by the institutional ethics committee of the University of Leipzig,

Germany (reference number 028–16–01022016). All data being used in here were collected in the routine transplant evaluation process.

Inclusion criteria consisted of RHC and [^{18}F]FDG-PET/ computed tomography (CT) scan, both performed within a time period of less than 1 year. In detail, the time interval between RHC and PET/CT averaged 1.5 $\pm$ 2.6 months, with a median of 0.4 months (0.2–1.7) as a result of its asymmetric, right-skewed, non-normal distribution. About 79% (86/109) of all patients underwent RHC and PET/CT imaging within 2 months.

The local lung transplant evaluation process requires among others a RHC and [^{18}F]FDG PET/CT for every patient being evaluated. Both examinations were carried out according to clinical indications.

The relative distribution of pulmonary disease was as follows: cystic fibrosis 3.7% (4/109), COPD 62.4% (68/109), ILD 30.3% (33/109, including asbestosis, hypersensitivity pneumonitis [HSP], idiopathic pulmonary fibrosis [IPF], idiopathic nonspecific interstitial pneumonia [NSIP], Langerhans cell histiocytosis [LCH], lymphangioleiomyomatosis [LAM], and sarcoidosis), and also PAH and CTEPH 3.7% (4/109; Table 1). Given the nature of this retrospective study, a healthy control group was not to be included. This circumstance may display a certain selection bias towards advanced pulmonary diseases comprising opposing parenchymal pathologies (emphysema vs interstitial lung diseases).

2.2. Hemodynamic, clinical, and laboratory data

Right heart catheterization provided data on mPAP given in mm Hg and PVR (dyn·s/cm^5, calculated by the following equation: PVR = [{mPAP – PCWP}/CO] × 80, where PCWP is pulmonary capillary wedge pressure and CO cardiac output). Patients with a resting mPAP $\geq$25 mm Hg were attributed to the group "pulmonary hypertension" according to the most recent clinical classification.[1] To discriminate severe PH, patients were grouped according to the PVR ($\geq$480 mm Hg).[12]

Data from 6-minute walking distance (6MWD) test, serum N-terminal pro-brain natriuretic peptide (NT-proBNP), C-reactive protein (CRP), and white blood cell (WBC) count were determined during the routine blood work-up at the same time of the PET/CT scan. NT-proBNP concentrations were transformed to the natural logarithm to the base e (lnNT-proBNP).

2.3. [^{18}F]FDG-PET/CT

All 109 patients were examined using a routine clinical protocol on an integrated PET/CT scanner (Biograph 16 PET/CT Scanner [Siemens Medical Solutions, Erlangen, Germany]). Patients were fasting for at least 12 hours. Sixty to ninety minutes after intravenous injection of a mean activity of 325 MBq (4 MBq or 108 μCi per kg body weight, range 224–426 MBq) [^{18}F]FDG, a whole body PET/CT scanning (from the vertex of the skull to the groin), was performed in a 3D-mode (3 minutes per bed position). According to clinical indication, a low-dose or a diagnostic CT was performed. If a diagnostic CT was indicated, a nonionic iodinated X-ray contrast agent (Imeron 400, Bracco Imaging, Konstanz, Germany) was applied. Dosing and imaging procedures used were in accordance with German and European PET/CT guidelines for tumor imaging.[13,14]

2.4. Image data analysis

The analysis of [^{18}F]FDG uptake was performed using the maximum and mean standardized uptake value (SUV$_{max}$ and

Table 1

Characteristics of 109 patients.

	n (%)	Age, yrs	Hemodynamic parameters			PVR	NT-proBNP
			mPAP				
			All patients	<25 (%)	≥25 (%)		
All patients	109 (100.0)	54.4 ± 7.5	29.1 ± 11.0	48 (44.0)	61 (56.0)	310.2 ± 279.4	755.2 ± 1614.2
Sex							
Male	66 (60.6)	54.9 ± 6.9	29.2 ± 11.5	28 (58.3)	38 (62.3)	299.8 ± 260.3	838.6 ± 1746.3
Female	43 (39.4)	53.7 ± 8.3	28.0 ± 10.6	20 (41.7)	23 (37.7)	326.0 ± 308.8	628.9 ± 1406.4
Cystic fibrosis	4 (3.7)	45.0 ± 16.6	30.3 ± 8.7	2 (4.2)	2 (3.3)	433.7 ± 246.7	288.9 ± 341.6
COPD	68 (62.4)	54.7 ± 6.8	25.4 ± 8.3	38 (79.2)	30 (49.2)	195.1 ± 120.9	526.8 ± 1402.7
ILD	33 (30.3)	55.3 ± 7.1	33.5 ± 11.5	8 (16.7)	25 (41.0)	428.8 ± 283.8	1026.2 ± 1666.1
Asbestosis	1 (0.9)	48	24	1 (2.1)	0 (0.0)	273	273.2
HSP	2 (1.8)	56.5 ± 6.4	33.7 ± 15.1	1 (2.1)	1 (1.6)	479.1 ± 335.3	2550.4 ± 3344.0
IPF	19 (17.4)	54.9 ± 8.4	31.2 ± 10.1	4 (8.3)	15 (24.6)	386.8 ± 320.8	780.3 ± 1424.3
NSIP	3 (2.8)	52.0 ± 4.4	25.7 ± 16.9	2 (4.2)	1 (1.6)	407.1 ± 310.3	93.8 ± 55.1
LCH	3 (2.8)	58.7 ± 7.1	46.3 ± 11.9	0 (0.0)	3 (4.9)	638.6 ± 105.9	692.8 ± 914.6
LAM	1 (0.9)	61	35	0 (0.0)	1 (1.6)	208	668.6
Sarcoidosis	4 (3.7)	56.8 ± 2.1	42.8 ± 6.4	0 (0.0)	4 (6.6)	556.3 ± 170.9	2290.4 ± 2550.1
PAH and CTEPH	4 (3.7)	52.0 ± 5.7	53.8 ± 7.6	0 (0.0)	4 (6.6)	1163.7 ± 341.8	769.9 ± 2545.7

COPD = chronic obstructive pulmonary disease, CTEPH = chronic thromboembolic pulmonary hypertension, HSP = hypersensitivity pneumonitis, ILD = interstitial lung disease, IPF = idiopathic pulmonary fibrosis, LAM = lymphangioleiomyomatosis, LCH = Langerhans cell histiocytosis, mPAP = mean pulmonary artery pressure (mm Hg), n = number, mean ± SD, NSIP = nonspecific interstitial pneumonia, NT-proBNP = N-terminal pro-brain natriuretic peptide (pg/mL), PAH = pulmonary artery hypertension, PVR = pulmonary vascular resistance (dyn·s/cm^5).

SUV_{mean}, respectively) of the region of interest (ROI), with the help of Hybrid-Viewer Software (Hermes Medical Solutions AB, Stockholm, Sweden) on co-registered PET/CT data: SUV_{mean} for lung parenchyma (LP), left (LV), and right ventricle (RV), and SUV_{max} for central left and right pulmonary artery (PA). Here, SUV_{max} was chosen for the PA to capture the vessel uptake of the PA rather than unspecific intraluminal blood pool activity. To access the SUV_{mean} of LP, ROIs were drawn in 3 different planes (3 ROIs in transverse and coronal, and 1 in sagittal plane) per lung (14 ROIs per patient lung) to calculate the mean value of the respective ROIs. The SUVs from the myocardium ROIs (LV, RV) and the right and left PAs were determined likewise in transverse plane (Fig. 1). The SUVs of each ROI were related to the SUV_{mean} of the volume of interest (VOI) of liver parenchyma resulting in SUV ratios (SUVRs). This semiquantitative analysis was performed to obtain a better comparability between the datasets. The distribution of CT-based attenuation correction with and without intravenous (i.v.) contrast enhancement was found to be equal among pulmonary diseases, mPAP, SUV_{max}, and $SUVR_{max}$ of the central PA, respectively. In detail, the respective distribution of i.v. contrast versus no contrast in COPD patients was as follows: 64.7% (44/68) of patients versus 35.2% (24/68), the mPAP was 24.5 versus 27.2 mm Hg, SUV_{max} 2.5 versus 2.3, and the $SUVR_{max}$ 1.1 versus 1.0. In ILD patients, the distribution of i.v. contrast versus no contrast was as follows: 63.6% (21/33) versus 36.4% (12/33), the mPAP was 37.8 versus 26.0 mm Hg, SUV_{max} 3.6 versus 2.7, and the $SUVR_{max}$ 1.3 versus 1.2.

2.5. Statistical analysis

The data were analyzed regarding normal distribution (D'Agostino–Pearson normality test). For data not normally distributed, a nonparametric Mann–Whitney U test determined group differences (mPAP < or ≥25 mm Hg, PVR < or ≥480 dyn·s/cm^5). Due to uneven distribution of NT-proBNP concentrations, these values were log-transformed to the base e (natural logarithm) to receive normal distribution. Regression analyses

with determination of the slope of the regression line ($y = f(x_i) = bx_i + a$; b = slope, a = intersection with y axis) were performed and the Pearson correlation coefficient r was calculated (r = covariance s_{xy}/[SD $s_x \times s_y$]). Statistical significance was accepted at a level of a 2-sided $P < 0.05$ and was illustrated with a linear regression line. Results are expressed as median with interquartile range (Q_{25}–Q_{75}), mean ± SD, or 95% confidence interval (CI). Data analysis, calculation, and preparation of figures were conducted using the software package GraphPad Prism version 5.03 (La Jolla, CA).

3. Results

3.1. Distribution of pulmonary hypertension in the study population

Fifty-six per cent (61/109) of patients with end-stage pulmonary disease presented with PH, with an mPAP ≥25 mm Hg at rest, of which 62.3% (38/61) were men and 37.7% (23/61) women (Table 1). Over 75% (25/33) of patients with ILD and about 44% (30/68) of patients with COPD were invasively measured with a resting mPAP ≥25 mm Hg. An elevated mPAP was found most frequently in ILD patients. These patients had the highest serum NT-proBNP compared with the other subgroups.

3.2. Group differences between [^{18}F]FDG uptakes in pulmonary hypertension

Patients with an mPAP ≥25 mm Hg (61/109) showed a significantly higher SUVR of LP ($P = 0.013$), PA ($P = 0.002$), RV ($P = 0.006$), and RV/LV ratio ($P = 0.049$) than patients with an mPAP <25 mm Hg (Table 2, Fig. 2A). Similar statistically significant group differences were found for patients with a PVR ≥480 dyn·s/cm^5: LP ($P < 0.001$), PA ($P < 0.001$), RV ($P = 0.045$), and RV/LV ratio ($P < 0.001$) (Fig. 2B). However, significant differences were found neither between SUVR of LV for mPAP nor for PVR ($P = 0.68$, $P = 0.26$, respectively).
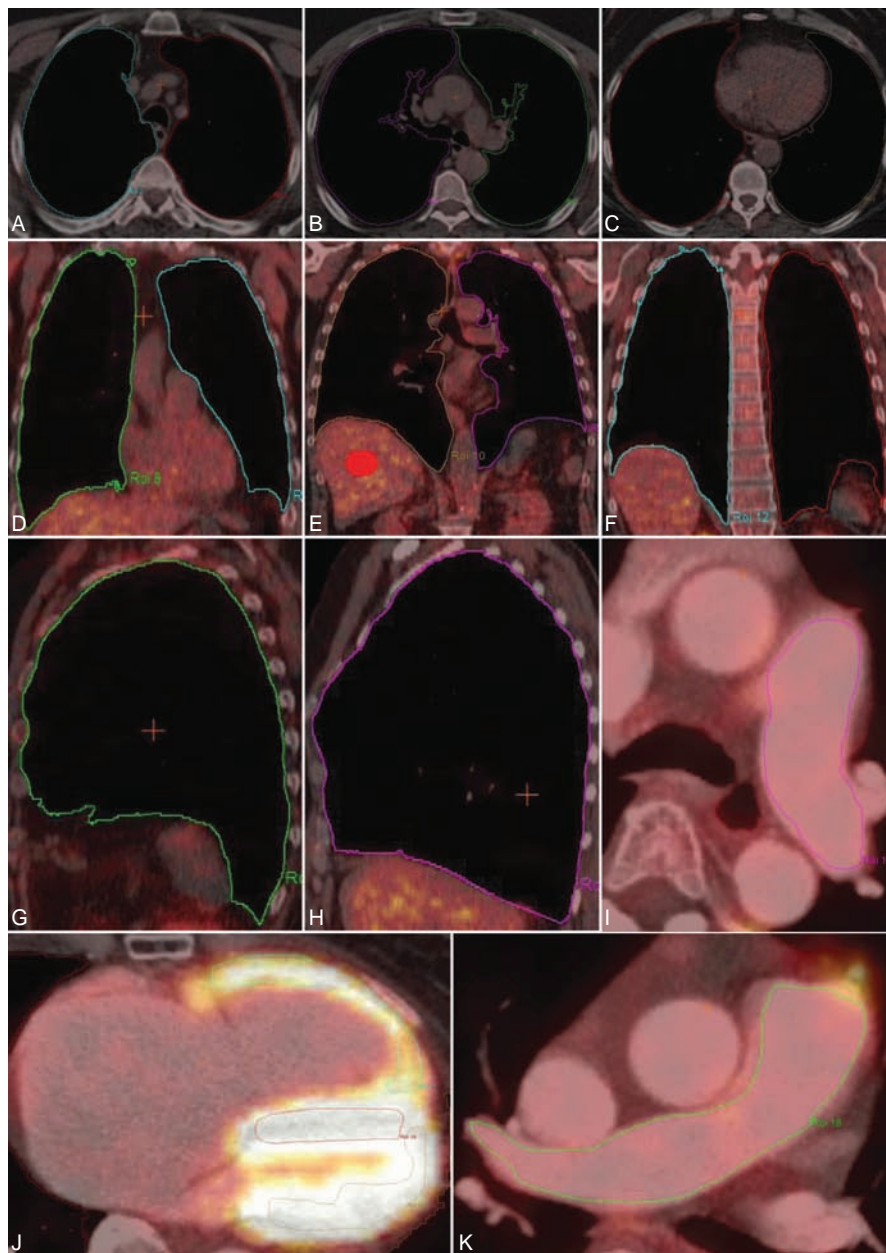
Figure 1. Exemplary overview of regions of interest (ROIs) delineated in [18F]FDG-PET/CT fusion images. ROIs of lung parenchyma in 3 different planes: transverse (A–C), coronal (D and F), and sagittal (G and H), of left (I) and right (K) central pulmonary artery, and also of left and right ventricular myocardium (J). Volume of interest (VOI) of liver parenchyma (E) as reference region for semiquantitative analysis. [18F]FDG-PET = [18F]fluorodeoxyglucose positron emission tomography, CT = computed tomography.

Table 2						
Group differences between [18F]FDG uptakes in 109 patients.						
	mPAP			**PVR**		
SUVR	**<25**	**≥25**	**P**	**<480**	**≥480**	**P**
n	48	61		88	21	
LP	0.15, 0.12–0.23	0.25, 0.14–0.42	0.013	0.16, 0.13–0.28	0.34, 0.24–0.42	<0.001
PA	1.04, 0.96–1.14	1.17, 1.00–1.33	0.002	1.07, 0.97–1.18	1.28, 0.16–1.39	<0.001
RV	0.61, 0.44–0.77	0.75, 0.54–1.37	0.006	0.63, 0.50–0.97	0.94, 0.57–1.99	0.045
LV	1.10, 0.55–2.68	1.27, 0.64–2.83	0.68	1.26, 0.64–2.98	0.75, 0.54–2.39	0.26
RV/LV	0.53, 0.31–0.79	0.73, 0.38–0.98	0.049	0.53, 0.31–0.85	0.88, 0.64–1.46	<0.001

LP = lung parenchyma, LV = left ventricle, mPAP = mean pulmonary artery pressure (mm Hg), n = number of patients, median with interquartile range, PA = pulmonary artery, PVR = pulmonary vascular resistance (dyn·s/cm⁵), RV = right ventricle, SUVR = standard uptake value ratio (SUV of each ROI normalized to SUV$_{mean}$ of VOI of liver parenchyma).
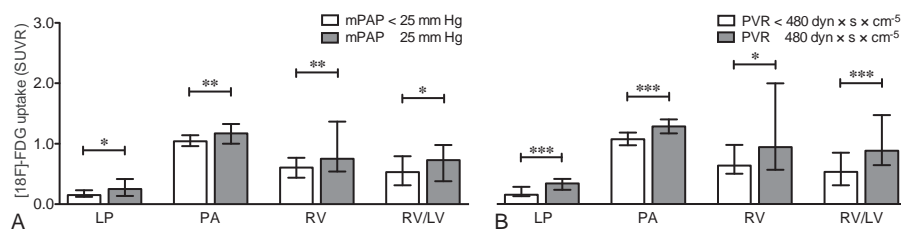
Figure 2. Significant group differences between pulmonary and right ventricular [18F]FDG uptake ratios (SUVRs) compared with the mean pulmonary artery pressure (A) and the pulmonary vascular resistance (B). Median with interquartile range. *$P < 0.05$, **$P < 0.01$, ***$P < 0.001$. [18F]FDG = [18F]fluorodeoxyglucose, LP = lung parenchyma, PA = pulmonary artery, RV = right ventricle, RV/LV = ratio of right to left ventricular myocardium.

3.3. Correlations between [18F]FDG uptake, mPAP, PVR, NT-proBNP, and 6MWD

In the study population of 109 patients with end-stage pulmonary disease, a positive linear correlation was found between mPAP, PVR, and NT-proBNP log-transformed, and the SUVR of LP, PA, and RV, respectively (Table 3, Fig. 3). The SUVR of LV did not correlate with mPAP, PVR, NT-proBNP, or 6MWD. 6MWD negatively correlated with SUVR of PA in ILD patients. Those correlations were not seen in COPD patients or in the total study population.

In subgroup analyses of COPD and ILD patients, those significant correlations were persistent: the mPAP correlated with the SUVR of PA and RV, but not the LP or LV (Table 3, Fig. 4).

3.4. Correlations between [18F]FDG uptake in LP, PA, and RV

The SUVR of PA positively correlated with both LP and RV in the study population ($r = 0.55$ with $P < 0.001$, $r = 0.42$ with $P < 0.001$, respectively) (Table 3, Fig. 5). Similar correlations were seen between LP and PA in the COPD but not in the ILD subgroup. Significant correlations between PA and RV were found in all subgroups (COPD: $r = 0.42$ with $P < 0.001$, ILD: $r = 0.53$ with $P = 0.002$).

3.5. Assessment of systemic inflammation in comparison with pulmonary [18F]FDG uptake and hemodynamic parameters

To distinguish between proliferation of the pulmonary vasculature from inflammation in patients with end-stage pulmonary diseases (COPD, ILD), CRP and WBC count were determined and compared with LP, PA, mPAP, and PVR (Table 4). Significant correlations were found between CRP and [18F]FDG uptake of LP or PA in the study population with a wide dispersion. No correlations were seen between CRP and [18F]FDG uptake of LP and PA, mPAP, or PVR in the subcohort of COPD and ILD patients. WBC count correlated with LP [18F]FDG uptake, but not with PA [18F]FDG uptake, in ILD patients. In the study subpopulation of COPD patients, WBC count did not correlate with [18F]FDG uptake of LP or PA, mPAP, or PVR.

4. Discussion

The purpose of this retrospective study was to investigate whether thoracic [18F]FDG uptake in lung parenchyma, PA, and myocardium depended on the presence and severity of PH in patients with end-stage pulmonary disease. The severity of PH was assessed by the mPAP and the PVR.

Pulmonary hypertension can be understood as an angioproliferative disease, which results in increased glucose utilization in the vessel wall cells and which may contribute to the disease process. Background seems a glycolytic shift towards aerobic glycolysis leading to increased glucose uptake, known as

Table 3

Correlation analysis.

Parameters	[18F]FDG uptake	n	Pearson r	95% CI	P
mPAP					
All patients	LP	109	0.29	0.10 to 0.45	0.0025
	PA	109	0.50	0.34 to 0.63	<0.001
	RV	109	0.39	0.22 to 0.54	<0.001
	LV	109	−0.02	−0.21 to 0.17	0.84
COPD	LP	68	0.21	−0.03 to 0.42	0.09
	PA	68	0.31	0.08 to 0.51	<0.01
	RV	68	0.36	0.13 to 0.55	0.003
	LV	68	0.04	−0.21 to 0.27	0.78
ILD	LP	33	−0.07	−0.41 to 0.28	0.69
	PA	33	0.56	0.26 to 0.76	<0.001
	RV	33	0.44	0.12 to 0.68	0.01
	LV	33	0.03	−0.32 to 0.37	0.87
PVR					
All patients	LP	109	0.35	0.17 to 0.51	<0.001
	PA	109	0.40	0.22 to 0.54	<0.001
	RV	109	0.35	0.17 to 0.50	<0.001
	LV	109	−0.08	−0.26 to 0.11	0.42
NT-proBNP					
All patients	LP	93	0.27	0.07 to 0.45	0.008
	PA	93	0.34	0.14 to 0.50	0.001
	RV	93	0.26	0.06 to 0.44	0.011
	LV	93	−0.06	−0.26 to 0.15	0.59
6MWD					
All patients	PA	107	−0.02	−0.20 to 0.18	0.88
COPD	PA	68	0.03	−0.21 to 0.27	0.79
ILD	PA	31	−0.37	−0.44 to 0.01	0.043
[18F]FDG uptake in LP					
All patients	PA	109	0.55	0.41 to 0.67	<0.001
	RV	109	0.15	−0.04 to 0.32	0.133
COPD	PA	68	0.49	0.28 to 0.65	<0.001
	RV	68	0.45	0.23 to 0.62	0.001
ILD	PA	33	0.30	−0.05 to 0.58	0.09
	RV	33	0.05	−0.30 to 0.38	0.79
[18F]FDG uptake in PA					
All patients	RV	109	0.42	0.25 to 0.56	<0.001
COPD	RV	68	0.42	0.21 to 0.60	<0.001
ILD	RV	33	0.53	0.22 to 0.74	0.002

[18F]fluorodeoxyglucose = [18F]FDG, 6MWD = 6-minute walking distance, CI = confidence interval, COPD = chronic obstructive pulmonary disease, ILD = interstitial lung disease, n = number of patients, NT-proBNP = N-terminal pro-brain natriuretic peptide depicted as natural logarithm to the base e.
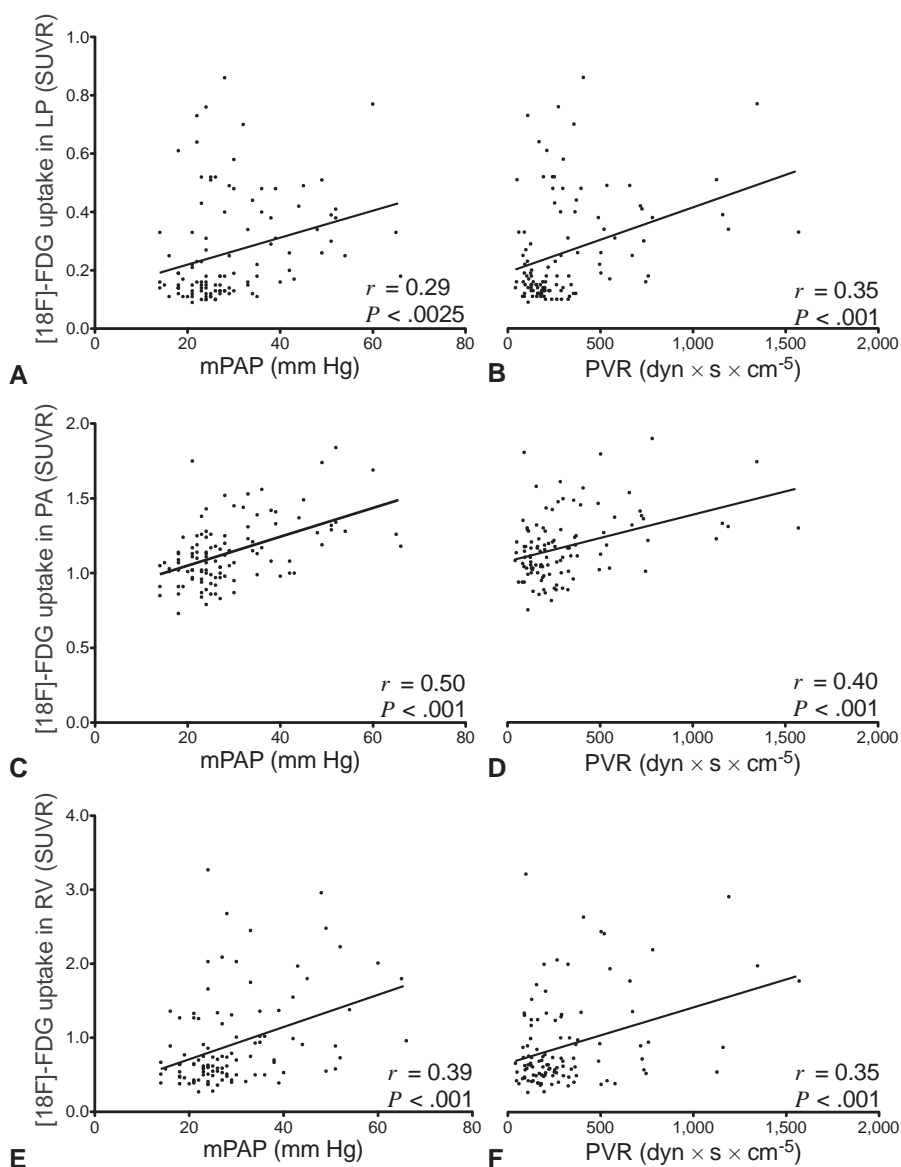
Figure 3. Positive correlations between [18F]FDG uptake in lung parenchyma (LP), central pulmonary arteries (PAs), right ventricle (RV), and hemodynamic parameters (mPAP, PVR). Scatterplots of standardized uptake value ratios (SUVRs) from 109 patients with pulmonary end-stage disease. Ordinate and labeling in the first column applies to each row, respectively. r represents Pearson correlation coefficient. [18F]FDG = [18F]fluorodeoxyglucose, mPAP = mean pulmonary artery pressure, PVR = pulmonary vascular resistance.

Warburg effect.[2,8] This increase of pulmonary glucose uptake can be quantified via [18F]FDG PET imaging.

Proliferation of endothelial and smooth muscle cells with thickening of intima and media of PAs in patients with COPD and IPF has already been reported in the context of pulmonary vascular remodeling.[15,16] We suppose that these mechanisms of pulmonary vascular remodeling in COPD and ILD patients with end-stage disease led to a measurable change in [18F]FDG uptake via PET imaging.

To our knowledge, very few studies investigated the pulmonary [18F]FDG uptake behavior in altogether 54 severely pulmonary hypertensive patients: 48 patients with PAH and 6 with CTEPH, with an average mPAP of 53.6 mm Hg and a PVR of 749.3 dyn·s/cm5.[5,9–11]

At the same time, cardiac alterations in glucose metabolism in PH have been investigated more extensively.[17–26] Together,

10 studies included 287 patients diagnosed with PH whereof 186 were with PAH, 75 with chronic heart failure, and 26 with CTEPH.

The strength of this study includes the considerably large number of patients investigated by RHC and [18F]FDG PET/CT. Patients were evaluated for lung transplantation due to end-stage pulmonary disease. The local lung transplant evaluation protocol strictly included a RHC and a [18F]FDG PET/CT. A certain selection bias therefore exists towards advanced pulmonary diseases with no healthy control group (emphysema vs interstitial lung diseases).

Dynamic acquisition of [18F]FDG via PET imaging principally allows measurements of functional glucose uptake in the lung in a time-dependent manner and its experimental modulation, for example, of glucose transporter 1.[9] It would provide a more in-depth analysis than static acquisition protocols as used in the
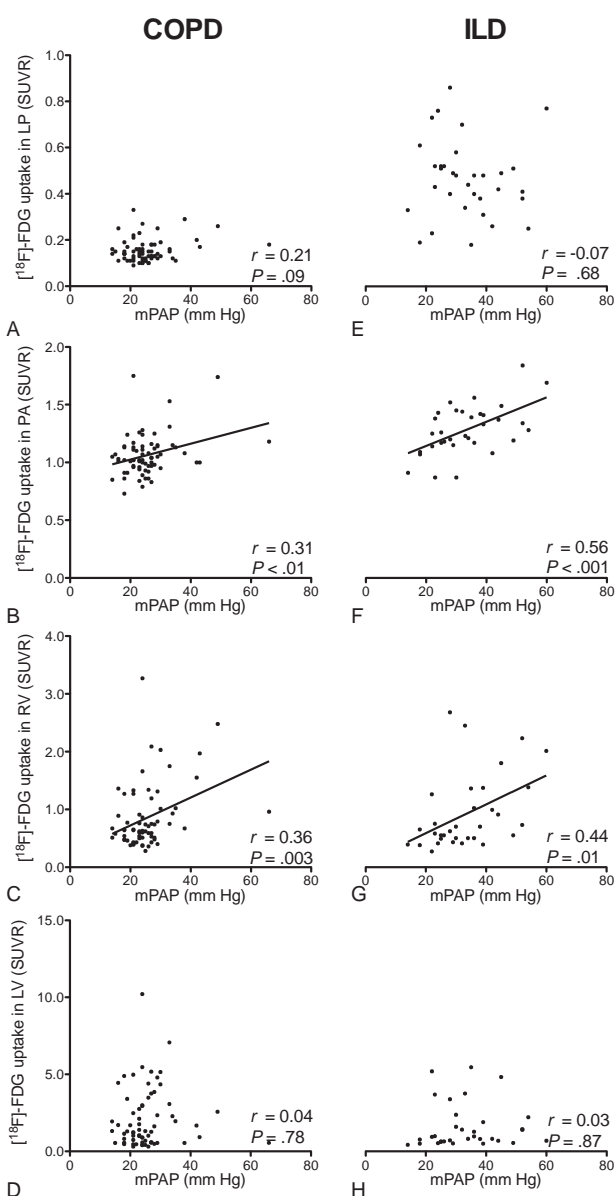
Figure 4. Subgroup analysis of 68 COPD and 33 ILD patients with positive correlations of [18F]FDG uptake in central pulmonary arteries (PAs), and right ventricle (RV) with mPAP. Ordinate and labeling in the first column applies to each row, respectively. *r* represents Pearson correlation coefficient. [18F]FDG = [18F]fluorodeoxyglucose, COPD = chronic obstructive pulmonary disease, ILD = interstitial lung disease, mPAP = mean pulmonary artery pressure.

present study.[9] Here, [18F]FDG PET/CT imaging was performed to rule out malignant diseases as part of the lung transplant evaluation process. Therefore, PET/CT was performed only with static acquisition using an approved routine oncologic protocol. Indeed, evaluation of glucose uptake in a routine PET/CT setup allowed us to investigate a large number of patients.

In the present study, subjects with PH due to end-stage pulmonary disease were investigated. [18F]FDG uptake in lung parenchyma, central PAs, and RV, but not in the LV, was significantly higher in patients with PH. In addition, the RV/LV uptake ratio was also elevated in PH patients. These patients suffered primarily from COPD and ILD (together 92.7%, 101/109), as illustrated in Table 1.

Concerning the pulmonary [18F]FDG uptake, Xu et al[5] and Zhao et al[9] separately demonstrated that pulmonary [18F]FDG uptake was significantly higher in 4 and 18 idiopathic pulmonary arterial hypertension (IPAH) patients than in 3 or 5 healthy comparators, respectively. In line with these results, Hagan et al[10] demonstrated increased [18F]FDG uptake in LP and in RV of 8 IPAH patients compared with 6 healthy controls, whereas [18F]FDG uptake in PA was not enhanced. However, here it is demonstrated that the [18F]FDG uptake in PA was significantly higher in patients with PH. These different results may be attributed to (1) a larger sample size (8/14 patients vs 61/109 patients) and (2) to different underlying pathophysiologic mechanisms (PH group 1 vs 3).

The severity of PH was assessed by mPAP, PVR, and NT-proBNP. These parameters are able to represent cardiopulmonary impairment and are of prognostic value.[1,27] A disease-specific stratification depending on glucose activity in the LP, the PA, the RV, or the RV/LV ratio as a surrogate parameter for patients with PH may be conceivable. [18F]FDG uptake in LP, PA, and RV, but not in LV, was found to positively correlate with mPAP, PVR, and serum level of log-transformed NT-proBNP in the study population. These correlations suggest that metabolic alterations in the lung, the PA, and the RV measured by [18F]FDG depended on PH severity. It is worth noting that the correlation between mPAP and the glucose uptake of the central PAs showed the strongest dependency of all correlations presented. Even subgroup analyses of COPD and ILD patients showed that glucose uptake of central PAs and the RV correlated positively with increased mPAP. Increased glucose uptake in the central PAs might be suggestive of severe PH and might be less affected by increased inflammatory processes of pulmonary diseases (COPD, ILD).

Interestingly, the SUVR of the central PAs positively correlated with the SUVR of both lung parenchyma and RV. This suggests that there may be a dependency of [18F]FDG uptake between the central PAs and the more peripheral pulmonary parenchyma, and also a right ventricular strain in terms of right ventricular dysfunction due to PH.

[18F]fluorodeoxyglucose positron emission tomography-imaging was shown to detect increased inflammation in COPD and even enhanced neovascularization in ILD patients.[28,29] In an attempt to distinguish between proliferative mechanisms of the pulmonary vasculature from the inflammatory nature of these end-stage pulmonary diseases (COPD, ILD), inflammatory parameters (CRP, WBC count) were determined and compared with glucose uptake in lung parenchyma, central PAs, and also hemodynamic parameters (mPAP, PVR). As expected, we found in all patients a significant correlation between [18F]FDG uptake in lung parenchyma and CRP. However, this correlation could not be reproduced in the subgroups of COPD and ILD patients, suggesting a weaker influence of inflammatory effects then PH on [18F]FDG uptake in lung parenchyma. Nevertheless, only in the ILD subgroup, WBC count correlated with the [18F]FDG uptake in the lung parenchyma, but not with the [18F]FDG uptake in the central PAs. In the latter, we found the strongest dependency on PH.

Untransformed NT-proBNP values showed a skewed distribution presumably due to different nature of PH, presence of acute exacerbation of pulmonary disease (COPD, ILD), or acute renal failure.[27,30] The log-transformation NT-proBNP data helped make the correlation clear with a more uniform dispersion. Indeed, these results are contrary to previous studies suggesting that pulmonary [18F]FDG uptake does not correlate
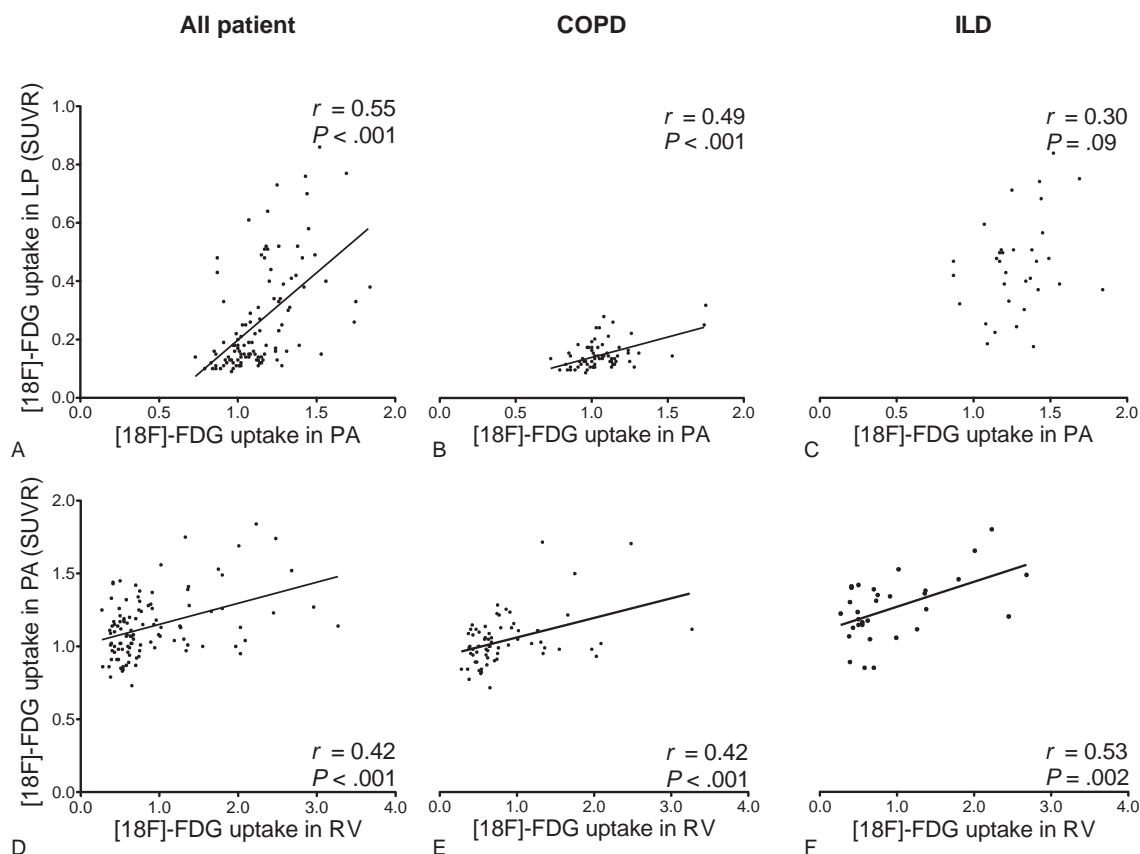
Figure 5. Positive correlations between [^{18}F]FDG uptake in central pulmonary arteries (PA) and lung parenchyma (LP) and right ventricle (RV) uptake. Scatterplots of standardized uptake value ratios (SUVRs) from 109 patients with pulmonary end-stage disease. Ordinate and labeling in the first column applies to each row, respectively. [^{18}F]FDG = [^{18}F]fluorodeoxyglucose, COPD = chronic obstructive pulmonary disease, ILD = interstitial lung disease, r = Pearson correlation coefficient.

with severity of PH in terms of mPAP, PVR, or NT-proBNP.[11] However, those data were collected from only 16 IPAH patients representing a different study population in terms of primary disease and smaller sample size compared with the present study.

In subgroup analyses of 4 PAH and CTEPH patients in this study, no significant correlations were found between the hemodynamic parameters and [^{18}F]FDG uptake in LP, PA, or RV (Supplemental Table 1, http://links.lww.com/MD/B52). This may be mostly due to the small sample size of 4 patients investigated.

In a previous study (Kluge et al[18]), the author's colleagues demonstrated that the [^{18}F]FDG uptake of the RV/LV ratio increased concordantly with the pulmonary arterial resistance in 30 patients with PH. Oikawa et al[17] reported data on 24 PH patients indicating an increased [^{18}F]FDG uptake in RV with increased PVR and mPAP. A positive correlation was seen between RV [^{18}F]FDG uptake and worse prognosis in PH patients in at least 3 clinical studies.[20,22,24] Our results are in line with these previous studies showing an increased glucose metabolism in the RV with increased PH.

The limitations of this retrospective study are attributed to a selection bias of patients with end-stage pulmonary disease because no healthy control group was included. Further, variations in the time interval between tracer injection and imaging due to the operational structure and workflow in a clinical routine PET/CT setting might have influenced the semiquantitative PET analysis. In addition, the maximal time interval between RHC and PET/CT imaging was a priori defined

as 1 year. The median time interval for all patients was 0.4 months (0.2–1.7), displaying a right-skewed, non-normal distribution. About 79% (86/109) of all patients underwent RHC and PET/CT imaging within 2 months. Generally, during regular trimonthly follow-up at the department outpatient clinic, there were no significant differences of the right heart function (e.g., mPAP) estimated in the transthoracic echocardiogram compared with the initial RHC data, indicating that no relevant clinical alteration occurred between RHC and PET/CT, and an adequate comparability was ensured.

Because the percentage of i.v. contrast applied during PET/CT was comparable between the groups of distinct pulmonary diseases, and neither the mean SUV nor the SUVR differed when contrast material was administered, we believe that the use of i.v. contrast was not a major confounder for SUV analysis in our study.

5. Conclusions

Pulmonary and cardiac [^{18}F]FDG uptake in PET imaging positively correlated with the presence and severity of PH in patients with end-stage pulmonary disease. Increased glucose metabolism in the central PAs seems to play a certain role in terms of severity of PH. These results suggest that [^{18}F]FDG-PET imaging can help understand the pathophysiology of PH as a proliferative pulmonary disease.

Nevertheless, the role of [^{18}F]FDG-PET imaging as a helpful tool in diagnosing PH and monitoring therapeutic effects still needs to be defined.

Table 4

Statistical analysis of systemic inflammation.

Parameters	[^{18}F]FDG uptake	n	Pearson r	95% CI	P
CRP					
All patients	LP	109	0.28	0.10 to 0.45	0.003
	PA	109	0.24	0.05 to 0.41	0.014
	mPAP	109	0.09	−0.10 to 0.27	0.38
	PVR	109	0.00	−0.19 to 0.19	0.99
COPD	LP	68	0.21	−0.04 to 0.42	0.09
	PA	68	0.04	−0.20 to 0.27	0.76
	mPAP	68	0.23	−0.01 to 0.44	0.06
	PVR	68	−0.01	−0.25 to 0.23	0.09
ILD	LP	33	0.24	−0.12 to 0.54	0.19
	PA	33	0.30	−0.05 to 0.59	0.09
	mPAP	33	−0.08	−0.41 to 0.27	0.67
	PVR	33	−0.12	−0.45 to 0.23	0.49
WBC count					
All patients	LP	108	0.34	−0.92 to 0.98	0.66
	PA	108	−0.95	−0.99 to 0.18	0.06
	mPAP	108	0.51	−0.89 to 0.99	0.49
	PVR	108	−0.05	−0.23 to 0.14	0.64
COPD	LP	68	−0.15	−0.37 to 0.10	0.23
	PA	68	−0.06	−0.30 to 0.18	0.60
	mPAP	68	0.12	−0.12 to 0.35	0.33
	PVR	68	0.15	−0.09 to 0.38	0.21
ILD	LP	32	0.47	0.15 to 0.71	0.006
	PA	32	−0.05	−0.40 to 0.30	0.77
	mPAP	32	−0.08	−0.42 to 0.28	0.66
	PVR	32	0.03	−0.32 to 0.38	0.87

CI = confidence interval, COPD = chronic obstructive lung disease, CRP = C-reactive protein, ILD = interstitial lung disease, LP = lung parenchyma, mPAP = mean pulmonary arterial pressure, n = number of patients, PA = central pulmonary arteries, PVR = pulmonary vascular resistance, WBC = white blood cell.

References

[1] Simonneau G, Gatzoulis MA, Adatia I, et al. Updated clinical classification of pulmonary hypertension. J Am Coll Cardiol 2013;62 (25 suppl):D34–41.

[2] Cool CD, Groshong SD, Oakey J, et al. Pulmonary hypertension: cellular and molecular mechanisms. Chest 2005;128(6 suppl):565S–71S.

[3] Bonnet S, Michelakis ED, Porter CJ, et al. An abnormal mitochondrial-hypoxia inducible factor-1alpha-Kv channel pathway disrupts oxygen sensing and triggers pulmonary arterial hypertension in fawn hooded rats: similarities to human pulmonary arterial hypertension. Circulation 2006;113:2630–41.

[4] Fijalkowska I, Xu W, Comhair SA, et al. Hypoxia inducible-factor1alpha regulates the metabolic shift of pulmonary hypertensive endothelial cells. Am J Pathol 2010;176:1130–8.

[5] Xu W, Koeck T, Lara AR, et al. Alterations of cellular bioenergetics in pulmonary artery endothelial cells. Proc Natl Acad Sci USA 2007;104:1342–7.

[6] Tuder RM, Davis LA, Graham BB. Targeting energetic metabolism: a new frontier in the pathogenesis and treatment of pulmonary hypertension. Am J Respir Crit Care Med 2012;185:260–6.

[7] Vander Heiden MG, Cantley LC, Thompson CB. Understanding the Warburg effect: the metabolic requirements of cell proliferation. Science 2009;324:1029–33.

[8] Pauwels EK, Sturm EJ, Bombardieri E, et al. Positron-emission tomography with [18F]fluorodeoxyglucose. Part I. Biochemical uptake mechanism and its implication for clinical studies. J Cancer Res Clin Oncol 2000;126:549–59.

[9] Zhao L, Ashek A, Wang L, et al. Heterogeneity in lung (18)FDG uptake in pulmonary arterial hypertension: potential of dynamic (18)FDG positron emission tomography with kinetic analysis as a bridging biomarker for pulmonary vascular remodeling targeted treatments. Circulation 2013;128:1214–24.

[10] Hagan G, Southwood M, Treacy C, et al. (18)FDG PET imaging can quantify increased cellular metabolism in pulmonary arterial hypertension: a proof-of-principle study. Pulmon Circ 2011;1:448–55.

[11] Ruiter G, Wong YY, Raijmakers P, et al. Pulmonary 2-deoxy-2-[(18)F]-fluoro-d-glucose uptake is low in treated patients with idiopathic pulmonary arterial hypertension. Pulmon Circ 2013;3:647–53.

[12] Hoeper MM, Andreas S, Bastian A, et al. [Pulmonary hypertension due to chronic lung disease. Recommendations of the Cologne Consensus Conference 2010]. Pneumologie 2011;65:208–18.

[13] Krause BJ, Beyer T, Bockisch A, et al. FDG-PET/CT in oncology. German Guideline. Nuklearmedizin 2007;46:291–301.

[14] Boellaard R, Delgado-Bolton R, Oyen WJ, et al. FDG PET/CT: EANM procedure guidelines for tumour imaging: version 2.0. Eur J Nuclear Med Molec Imaging 2015;42:328–54.

[15] Farkas L, Gauldie J, Voelkel NF, et al. Pulmonary hypertension and idiopathic pulmonary fibrosis: a tale of angiogenesis, apoptosis, and growth factors. Am J Respir Cell Mol Biol 2011;45:1–5.

[16] Barbera JA. Mechanisms of development of chronic obstructive pulmonary disease-associated pulmonary hypertension. Pulmon Circ 2013;3:160–4.

[17] Oikawa M, Kagaya Y, Otani H, et al. Increased [18F]fluorodeoxyglucose accumulation in right ventricular free wall in patients with pulmonary hypertension and the effect of epoprostenol. J Am Coll Cardiol 2005;45:1849–55.

[18] Kluge R, Barthel H, Pankau H, et al. Different mechanisms for changes in glucose uptake of the right and left ventricular myocardium in pulmonary hypertension. J Nuclear Med 2005;46:25–31.

[19] Mielniczuk LM, Birnie D, Ziadi MC, et al. Relation between right ventricular function and increased right ventricular [18F]fluorodeox-

yglucose accumulation in patients with heart failure. Circ Cardiovasc Imaging 2011;4:59–66.

[20] Can MM, Kaymaz C, Tanboga IH, et al. Increased right ventricular glucose metabolism in patients with pulmonary arterial hypertension. Clin Nucl Med 2011;36:743–8.

[21] Bokhari S, Raina A, Rosenweig EB, et al. PET imaging may provide a novel biomarker and understanding of right ventricular dysfunction in patients with idiopathic pulmonary arterial hypertension. Circ Cardiovasc Imaging 2011;4:641–7.

[22] Fang W, Zhao L, Xiong CM, et al. Comparison of 18F-FDG uptake by right ventricular myocardium in idiopathic pulmonary arterial hypertension and pulmonary arterial hypertension associated with congenital heart disease. Pulmon Circ 2012;2:365–72.

[23] Wang L, Zhang Y, Yan C, et al. Evaluation of right ventricular volume and ejection fraction by gated (18)F-FDG PET in patients with pulmonary hypertension: comparison with cardiac MRI and CT. J Nucl Cardiol 2013;20:242–52.

[24] Tatebe S, Fukumoto Y, Oikawa-Wakayama M, et al. Enhanced [18F] fluorodeoxyglucose accumulation in the right ventricular free wall predicts long-term prognosis of patients with pulmonary hypertension: a preliminary observational study. Eur Heart J Cardiovasc Imaging 2014;15:666–72.

[25] Lundgrin EL, Park MM, Sharp J, et al. Fasting 2-deoxy-2-[18F]fluoro-D-glucose positron emission tomography to detect metabolic changes in pulmonary arterial hypertension hearts over 1 year. Ann Am Thorac Soc 2013;10:1–9.

[26] Yang T, Wang L, Xiong CM, et al. The ratio of (18)F-FDG activity uptake between the right and left ventricle in patients with pulmonary hypertension correlates with the right ventricular function. Clin Nucl Med 2014;39:426–30.

[27] Leuchte HH, El Nounou M, Tuerpe JC, et al. N-terminal pro-brain natriuretic peptide and renal insufficiency as predictors of mortality in pulmonary hypertension. Chest 2007;131:402–9.

[28] Jones HA, Marino PS, Shakur BH, Morrell NW. In vivo assessment of lung inflammatory cell activity in patients with COPD and asthma. Eur Respir J 2003;21:567–73.

[29] El-Chemaly S, Malide D, Yao J, et al. Glucose transporter-1 distribution in fibrotic lung disease: association with [(1)(8)F]-2-fluoro-2-deoxyglucose-PET scan uptake, inflammation, and neovascularization. Chest 2013;143:1685–91.

[30] Leuchte HH, Baumgartner RA, Nounou ME, et al. Brain natriuretic peptide is a prognostic parameter in chronic lung disease. Am J Respir Crit Care Med 2006;173:744–50.